Inverse problems: deriving hidden information from what we see

Emily Mekireche - Luca Ponzano Andrade - Anais Guellaff - Sofien Fiess

Mijail Littin

June 15, 2024

Contents

1 Introduction **4**

2 Definition **5**

2.1 Inverse and forward problems . . . 5

2.2 Well-posed and Ill-posed problems . . . 5

3 Examples and applications **6**

3.1 Seismology . . . 6

3.2 X-ray tomography . . . 6

3.3 Image restoration . . . 7

3.4 Example of a type of inverse problem: "The Deconvolution method" . . . 7

3.4.1 Convolution and Deconvolution: . . . 7

3.4.2 Soot temperature Measurements . . . 8

4 State of the art **9**

4.1 Flame: . . . 9

4.2 Laminar flame . . . 9

4.3 Soot: . . . 10

4.4 Blackbody (Plancks law): . . . 10

4.5 Soot temperature: . . . 11

5 Unfolding of the project **12**

6 The experiment **13**

6.1 Introduction and details . . . 13

6.2 Experimental protocol: . . . 13

7 Interpretation of the data **17**

8 Uncertainties **20**

9 Conclusion **22**

10 Acknowledgments **22**

1 Introduction

Humanity has always been driven by the pursuit of solutions to various challenges. At the heart of this pursuit lies the essence of problem-solving. Traditionally, problems have been approached in a direct way, starting with identifying causes and then deducing their effects. However, an alternative called the "inverse problem" has emerged[6].

The inverse problem represents a departure from conventional problem-solving methods. Rather than beginning with causes and proceeding to effects, the inverse problem starts with observed effects and seeks to elucidate their underlying causes. This shift in perspective has profound implications, specially in scientific research.

In science, our observations are often constrained by limitations in technology or instrumentation. Consider, for example, capturing an image of a black hole. Despite our technological advancements, the resulting image remains imperfect due to the limitations of telescopes and imaging techniques. Such constraints necessitate the reconstruction of images from incomplete or imperfect data, presenting a classic example of an inverse problem.

Several methods have been developed to tackle inverse problems. One approach is to combine data from multiple observations to better understand the overall situation. For example, by using data from different angles or using various types of sensors, we can piece together a more complete and accurate picture of the phenomenon under study. Additionally, mathematical techniques and models are invaluable for solving complex inverse problems by providing frameworks and tools to interpret the data accurately.

A notable application of inverse problems is on the reconstruction of a local property from its line-of-sight measurements. This technique is especially useful in fields like combustion research. The Abel inversion, named in honor of Niels Abel, enables the reconstruction of a radial or local property in an axisymmetric flame. One approach to proceed is the Onion-Peeling technique. This approach sequentially removes outer layers of data to reveal the underlying structure, much like peeling an onion.

In this document, we explore the world of inverse problems in scientific research. By looking at different methods and real-world examples, we hope to show just how important this approach is for advancing our understanding of the natural world.

2 Definition

2.1 Inverse and forward problems

An inverse problem can be better understood by explaining what a "forward problem" is [8].

A forward problem involves having an input, represented as a set of parameters describing a physical model. These parameters then enter a system, which is the physical theory used to predict the outcome. Finally, we have an output, which is simply the result and is always accompanied by errors.

The topic to be discussed in this document is the opposite of this. As previously stated, an inverse problem is about knowing hidden information from external measurements. Therefore, the output is known, accompanied by errors, and our task is, from this latter, to determine either the system (physical theory) or the parameters describing the output.

We can express the above-described scenario as:

$$m \longrightarrow f(m) \longrightarrow d + A$$

Where m represents the parameters, which are introduced into a system f and which gives as output d and the associated errors A. Therefore, an inverse problem is determining m or f from $d + A$.

2.2 Well-posed and Ill-posed problems

A problem can be formulated in such a way that it verifies certain conditions. We define the following concepts:

We are dealing with a "Well-posed problem" if:

1. A solution exists (it gives the "existence")
2. The solution is unique (it gives the "uniqueness")
3. The solution depends continuously on the BC/IC (boundary conditions or/and initial conditions) (it gives the "stability")

If one of these conditions is not verified, then it is called an "ill-posed problem", which is more difficult to deal with due to obvious issues, such as the need to periodically reformulate the problem, add more constraints or the lack of information, among other factors.

3 Examples and applications

[5]

3.1 Seismology

In seismology, the inverse problem's goal is to deduce the physical characteristics of the subsurface by analyzing seismic measurements. A generic formulation would be the following:

Seismic⟶Layers⟶Reflection

Here, the seismic waves are going through the layers of the earth and what we measure are the reflections of them. Eventually the goal is to know the models of those seismic waves or to know where these layers are. Another point of view in this field would be just by identifying properties of a knowed seismic wave. By describing a seismic wave as follows:

$$\partial 2tp(t,x) - c(x) \bigtriangledown xp(t,x) = q(t,x), x\epsilon\Omega, t\epsilon[0,T] \quad (1)$$

Where c(x) is related to the speed of sound and density of the medium and q(t,x) the source. The properties of interest by using an inverse problem would be c or q, retrieved by some measurements of the function p(t, x).

3.2 X-ray tomography

In the field of medicine, X-rays are frequently used to provide a detailed image of a patient's anatomy. A generic formulation in this area would be the following:

X-ray Source⟶Object⟶Damping

In this case we know the input (X-ray source) and the output (the X-rays that come out and the corresponding damping), therefore the objective of the inverse problem would be to know the object that gives the damping. Here, the X-ray transformations are equivalent to the Radon transformations, which are sinograms obtained by integrating at different angles of the object's density. This sinogram is the following:

$$f(s,\xi) = \int u(s+t\xi)dt \quad (2)$$

Where f is the sinogram function and u the density of the image. Here, the inverse problem's goal is to get the image from the sinogram.

3.3 Image restoration

One of the most common reverse problems we can think of is restoring an image, the general setting in this situation is the following:

Scenery⟶lens⟶image

Here, we send the light (input) through the lens (system) and we get as an output a blurry and noisy image. In this case, the output is well known and by modeling the lens-associated blur mixing it with image restoration, we perfectly know the system so with these two data we could find out the sharp image.

3.4 Example of a type of inverse problem: "The Deconvolution method"

[1]

3.4.1 Convolution and Deconvolution:

Convolution: it is a mathematical operation that joins two functions (understood as two signals) to create a third. These functions are related by a sum of one function, after having been modified by the other. Deconvolution: it is precisely the "inverse problem" of a convolution, that is, inverting the convolution operation to obtain the original signal.

Application for image restoration: If we consider an image or photograph, the convolution formula in 2D dimension is defined as:

$$(IxK)[i,j] = m\sum n\sum I[i+m,j+n]K[m,n] \tag{3}$$

Where,

- I: original image (set of pixels)
- K: the blur effect, the lens filter, etc. Called convolution nucellus
- $(IxK)[i,j]$: the pixel value of the original image after applying the convolution nuceloi at position [i,j]
- $I[i+m,j+n]$: values of the original image at each position
- $K[m,n]$: kernel value (blur effect) at position [m,n]

With this sum, we obtain the value of each pixel after applying the convolution, that is, the resulting image. Knowing the filter, deconvolution would approximate the value of I[i,j], that is, knowing the image without a filter.

3.4.2 Soot temperature Measurements

How is the temperature of soot measured according to two wavelengths?

This goal is achieved by coupling flame emission measurements at two wavelengths (or more) in the visible and near-infrared spectrum. Thus, we can obtain different properties of soot, and among these, the temperature at different pairs of wavelengths detection[4, 11]. The "two-color pyrometry (2C)" method is used and we assume the following statements:

- Soot is in thermal equilibrium with the gas in the flames.
- Soot particles behave as a black body

Now, according to the following formula the temperature is obtained at each wavelength .

$$T_{2C,\lambda_1-\lambda_2} \approx \left(\frac{k_b}{hc\left(\lambda_1^{-1} - \lambda_2^{-1}\right)} \ln\left(\frac{J_{\lambda_2}}{J_{\lambda_1}} \left(\frac{\lambda_2}{\lambda_1}\right)^6 \right) \right)^{-1}, \tag{4}$$

Where,

- k_b: Boltzmann constant
- h: Plank constant
- c: speed of light
- λ: the given wavelength
- J: Abel inverted local thermal emission rate

4 State of the art

4.1 Flame:

A flame, derived from the Latin word "flamma", constitutes the observable, gaseous segment of a fire, resulting from an intensely exothermic chemical reaction occurring within a narrow zone [2]. When flames reach high temperatures, leading to the ionization of gaseous elements with adequate density, they transition into what is known as plasma, though this distinction can sometimes be imprecise. The color and temperature of a flame vary depending on the fuel used in combustion. The intense heat of the flame causes vaporized fuel molecules to break down, forming various incomplete combustion by-products and free radicals. These substances then interact with each other and with the oxidizer present in the combustion process. Water vapor, resulting from combustion, dominates the higher regions of the flame, while the yellowish middle portion typically contains soot.

Besides oxygen, various oxidizers can be employed to produce a flame. Different methods exist for distributing the necessary components of combustion to a flame. In a diffusion flame, which is the type of flame we are going to work on, oxygen and fuel diffuse into each other, igniting where they meet. In contrast, a premixed flame involves the mixing of oxygen and fuel before ignition, resulting in a different flame type. For instance, candle flames, which are diffusion flames, operate through the evaporation of fuel. The evaporated fuel rises in a laminar flow of hot gas, mixes with surrounding oxygen, and then combusts.

4.2 Laminar flame

A laminar flame is a type of flame characterized by smooth, orderly flow of reactants and combustion products [3]. In a laminar flame, the reactants (fuel and oxidizer) mix gradually and uniformly, resulting in a flame front that moves in a well-defined and relatively steady manner. This type of flame typically occurs under conditions where the flow velocity is low and the mixing between fuel and oxidizer is limited.

Laminar flames are often distinguished by their distinct appearance, with a clearly defined flame front and minimal turbulence within the flame. They can be observed in various combustion systems, such as laboratory experiments, certain types of burners, and some industrial processes.

In contrast, turbulent flames exhibit irregular mixing of reactants and combustion products, resulting in chaotic flame fronts and enhanced heat and mass transfer. Turbulent flames are common in many practical combustion applications, including engines, furnaces, and wildfires.

Laminar diffusion flames are attractive for research because they offer simplified flame models, easier to analyze and experiment with compared to turbulent flames. They provide valuable insights into combustion processes and serve as a foundation for developing computational models applicable to more complex scenarios.

4.3 Soot:

Soot is a dark, powdery substance primarily composed of carbon, formed when organic materials undergo incomplete combustion. It often results from the burning of fuels like wood, coal, oil, or gas. Soot exposure has been linked to various cancers and lung diseases.

4.4 Blackbody (Plancks law):

Planck's law[7] is a fundamental principle in physics that describes the spectral density of electromagnetic radiation emitted by a blackbody at a given temperature. A blackbody is an idealized physical body that absorbs all incident electromagnetic radiation, regardless of frequency or angle of incidence, and emits radiation thermally in accordance with its temperature.

Planck's law states that the spectral radiance of a blackbody per unit wavelength, $B(\lambda, T)$, is given by:

Equation 5

$$B(\lambda, T) = \frac{2hc^2}{\lambda^5} \frac{1}{e^{\frac{hc}{\lambda k T}} - 1} \tag{5}$$

Where:

- $B(\lambda, T)$ is the spectral radiance at wavelength λ and temperature T.
- h is the Planck constant
- c is the speed of light in a vacuum
- k is the Boltzmann constant
- T is the temperature of the blackbody in Kelvin
- e is the base of the natural logarithm

This formula essentially tells us how much energy a blackbody emits at each wavelength for a given temperature. It's important to note that as temperature increases, the peak wavelength of emission shifts to shorter wavelengths (higher frequencies), and the total emitted radiation increases.

In essence, a blackbody serves as a theoretical construct to understand and model the behavior of thermal radiation. While true blackbodies do not exist in nature, many objects, such as stars and even everyday objects at high temperatures, can closely approximate blackbody radiation.

4.5 Soot temperature:

[9]

Soot temperature varies at a function of time, it can have different values throughout the phenomenon of combustion.

First of all, there is the formation temperature, which corresponds to the temperature at which the soot particles start forming during incomplete combustion. This soot formation usually happens at high temperatures as the fuel molecules break down into smaller fragments that turn into soot particles. The formation temperature can be influenced by different factors such as the fuel or the combustion conditions.

Secondly, we can also have the oxidation temperature. That is the temperature at which the soot particles are oxidized or burned off. The oxidation temperature often has elevated values and it is thus an important factor to take into account when wanting to reduce soot emissions in order to improve combustion efficiency.

Finally, we have the measurement temperature, which is the value measured during the experimental procedure. This value can be different from the actual soot temperature depending on the precision and the time of the experiment. Indeed, measurement errors due to instrument limitations or spatial and temporal variations in the flame can occur.

To give an experiment application, soot temperature can be found by using the "two color pyrometry (2C)" method:

By coupling flame emission measurements at different wavelengths in the visible and near-infrared spectrum, we can obtain different properties of soot, and among these, the temperature at different pairs of detection wavelengths. Although, in doing so, different statements have been assumed:

- Soot is in thermal equilibrium with the gas in the flames
- Soot particles behave as a black body

Therefore, the reason for adopting this procedure and not another alternative is because this method is not intrusive, since the dynamics of the particles in the flame are not altered.

5 Unfolding of the project

Planck's law describes the spectral radiance of a black body at a given temperature as a function of wavelength. While Planck's law itself doesn't directly provide a way to retrieve the temperature of a flame, it can be used after certain experimental measurements of a flame's spectral radiance in order to deduce its temperature.

Here's the approach we are going to take:

The experiment: We will use a camera to capture images of a laminar flame at a given wavelength.

→This will give us a 2D photograph of the flame

From the previous photograph, we will use informatics programming tools (Python) to create a set of data points representing the intensity of radiation emitted by the flame at the particular wavelength.

→This will give us a graph (x,I)

Thanks to that graph, we will be able to exploit the Abel Inversion method, which will let us obtain a new graph representing the radial distribution of the intensity of the flame as a function of radial distance from the flame center.

→ This will give us a graph (y,K(r))

Finally, given that last graph, we will use Planck's law and mathematical tools in order to deduce the temperature of the flame.

All these steps will be applied twice, at 2 different wavelengths so we get more precise results we will be able to compare.

It's important to note that this method relies on the assumption that the flame behaves approximately like a black body radiator, which may not always be the case. Indeed, a flame's emission spectrum may closely resemble that of a black body, especially if the flame is sufficiently hot and the surrounding environment is relatively uniform. In such cases, certain properties of the flame's radiation emission may exhibit behavior similar to that of a black body, but it would still not meet the strict definition of a black body. Additionally, the accuracy of the temperature determination depends on factors such as the accuracy of the measurement system, the validity of the Abel inversion technique, and the spectral characteristics of the flame. Therefore, careful validation and calibration are necessary to ensure accurate results.

We could also, to obtain even more information, analyze the soot particles emitted by the flame.

6 The experiment

6.1 Introduction and details

The aim of this experiment is to perform optical measurements in a well-controlled environment. We are going to capture a picture of a diffusion flame, which is a flame in which the oxidizer and fuel (we are using ethylene) are separated before burning. In order to obtain precise information for our further research, we will take 100 different images of the flame at 2 different wavelengths: 640 and 750 nm.

We need these 2 wavelengths because Planck's law is related to the black body with the temperature and the wavelength. By getting the data at different wavelengths we will be able to determine the temperature of the flame.

It can also be noted that if we had also made the experiment with a laser, we would have been able to measure the attenuation light which would have given us the number of particles in the flame. We are unable to proceed with this experiment as we do not have the required equipment. The data we are going to collect will only allow us to determine the soot temperature.

Moreover, it is important to note that the flame we are going to photograph has to be perfectly parallel, axisymmetric and stabilized in the aim of getting the precise information we need for the processing of our results. As we only want to capture using one color, we are going to use a filter in order to cancel out the information linked to all the other colors we will not be using.

The experiment has been prepared in advance, so the calibration of the devices has already been made. Our need of capturing all the signals parallel to the lens requires that the installation needs to be perfectly parallel. The height of the different devices has been modified to this effect.

It is also useful to note that the light in the room does not affect our experiment because the signal is being filtered and all the measurements are made in the same conditions. On the other hand, it is required that we do not move during the time of the measurements as any kind of movement could disturb the signals.

6.2 Experimental protocol:

We started off by turning on the light and setting the mass flow of the ethylene and air, as shown on the following images.

Figure 1: Images of the air and ethylene mass flow controllers

Then, we switched on the gas along with the flame with a Gülder burner (useful to obtain a laminar flame). Once the flame started burning, we turned on the exhaust as the flame emits soot carbon particles which can be dangerous to be breathed in.

Figure 2: Images of the ethylene bottle, the Gulber Burner and the exhaust

We then started using the camera, for which we had to adjust the gain (the amount of power used to amplify the signal) and the exposure time.

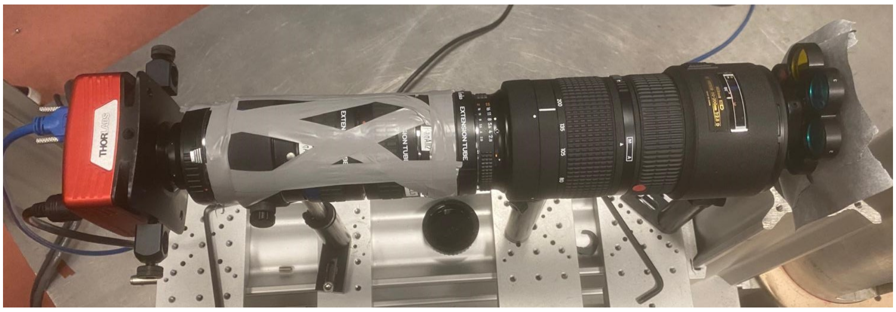

Figure 3: Image of the Nikon camera used during the experiment

We started off by capturing black and white images of the flame at 640 nm. It was first of all more or less stable, but as the movement affects the measurements, we placed a transparent quartz tube around the flame which stabilized it.

After that, we obtained a motionless flame, but this tool added a reflection to the data we were collecting, which we could see on the first part of the graph presented by the computer. Also, we knew our flame needed to be axisymmetric, but the graph showed a greater intensity on its right part (seen on the peaks of the graph) and unwanted effects due to the reflections of the transparent tube (seen on the corners of the graph). After taking into account these 2 errors in our graph, we solved the reflection and then the

Figure 4: Image of the Burner and the added tube

symmetry by turning the flame around. We were then in the right conditions to take the 100 images and the measurements at the 640 nm wavelength.

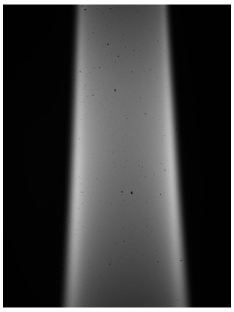

Figure 5: Example of one image taken by the camera at 640nm

After that, we changed the wavelength to 750 nm. At first, we obtained a non-usable signal as it was a larger wavelength, the graph was saturating and there was as a consequence no symmetry. To resolve this matter we changed the setup on the camera by adjusting the exposure to 35 ms and moved the tube. An adjustment on the gain was not required. We finally rotated the flame in order to obtain a symmetrical image and took the measurements for the 750 nm wavelength.

With a view to only get a picture of the flame without its environment, we also had to record the background, which consists of the image setup without the flame. We thus turned off the flame and made the background images for the 2 different wavelengths. Thanks to these 2 new pictures, we will be able to substract the background on our initial measurements.

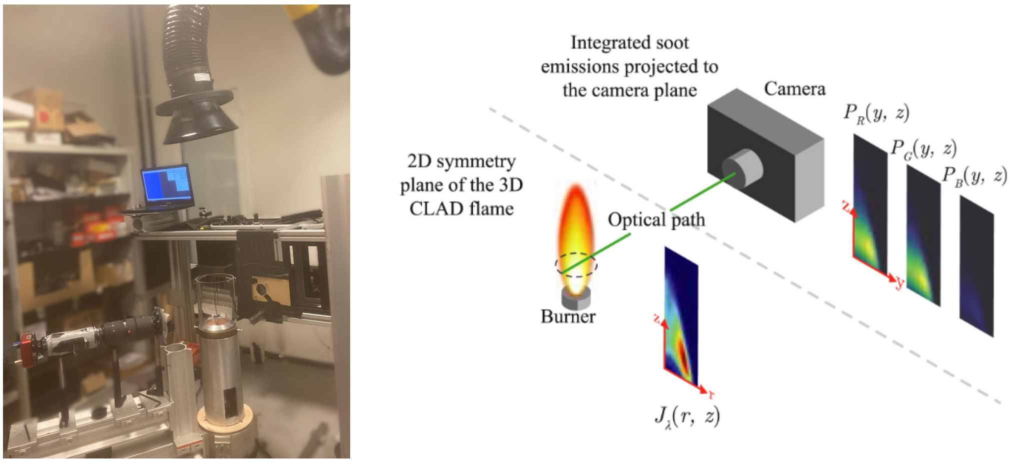

Figure 6: Image and sketch of the experimental setup

Parameters of the experiment :

Exposure: 640 nm: 100 ms
750 nm: 75 ms
Gain: 640 nm: 54
750 nm: 54
Resolution: 185 px per mm
Mass flow: Ethylene : 0.194 L/min
Air : 150 L/min
Pixel number: 3296*2144 pixels
Burner name: Gulber
Camera brand: Thorlabs
Lens brand: Nikon-200 mm

In the aim of making our experiment clear to any reader, we are requested to give a reference concerning the size of the flame we are capturing. Indeed, the flame has a physical meaning and we are using pixels, which does not give any information about the size of the burner. In response to this issue, we need to calibrate by counting the number of pixels per mm. To do this, we photographed a grid, knowing each square corresponded to 1.5 mm and we counted the number of pixels.

We can also mention at the end of this experiment that we could make measures with a different angle, which would allow us to measure the attenuation with the scattering light according to the size of the particles. These particles can be characterized with optical measurements, and the angle can be controlled by the computer. (In our case, with a linear installation, the attenuation can be estimated by volume fraction.)

7 Interpretation of the data

[10] After our experiment, we have captured a projection of the flame, which is a 3D object. We thus need to convert our observations into spatial data or else it will not be complete information. Indeed, the imaging camera receives all the light from the flame, but it can only represent it in a 2D view. Therefore, we need to reconstruct the image captured by the camera in 3D: this is the Abel problem. In order to do this we will use PyAbel, a Python package that provides functions for the Abel transforms. PyAbel includes different transform methods. The one that we will use here is the onion-peeling method. This means we will sequentially remove outer layers of data to reveal the underlying structure of the flame.

After applying the onion-peeling method in the inverse way, it gives us a deconvoluted image of the flame at the two different wavelengths. The standard resolution is 3296*2144 pixels but the flame have a symmetry in its center so we reduced it in half. We also changed the unit to mm. This image starts from 20mm and goes up to 38mm in order to only see the interesting part.

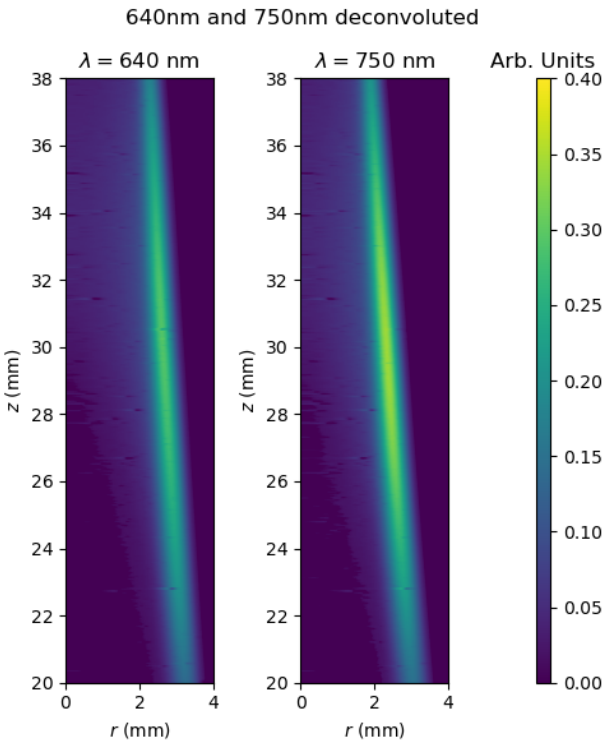

Figure 7: 2D image of the flame at the two different wavelengths

In the aim to maximize the precision of our graphs, we calculated the mean and the standard deviation of the 2D images, as seen in the following figures.

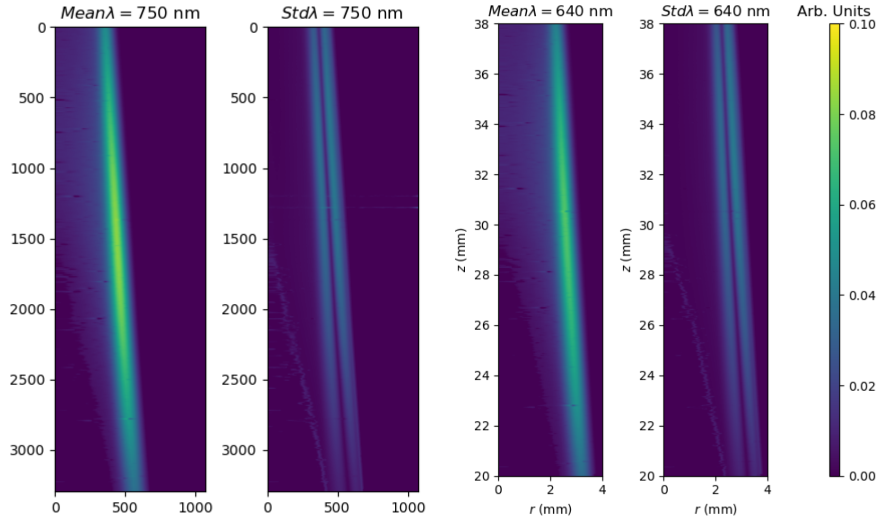

Figure 8: Mean and Standard Deviation at 750nm and 640nm

After a calibration, we can now deliver the emission (J(λ)) of the flame at two different wavelengths.

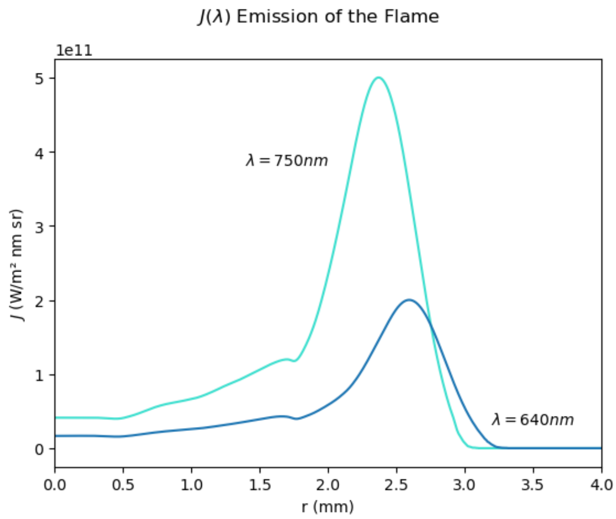

Figure 9: Emission $J(\lambda)$

We can perceive a peak in approximately 2.5mm which corresponds to the part right before the wing of the flame. Furthermore, we can notice that the curve at 750nm is almost two times higher than the one at the 640nm wavelength.

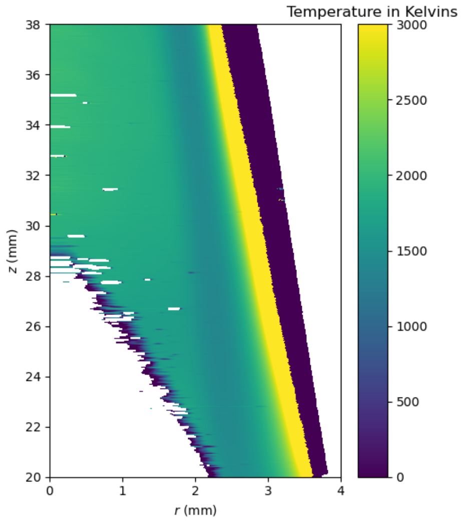

Figure 10: Temperature

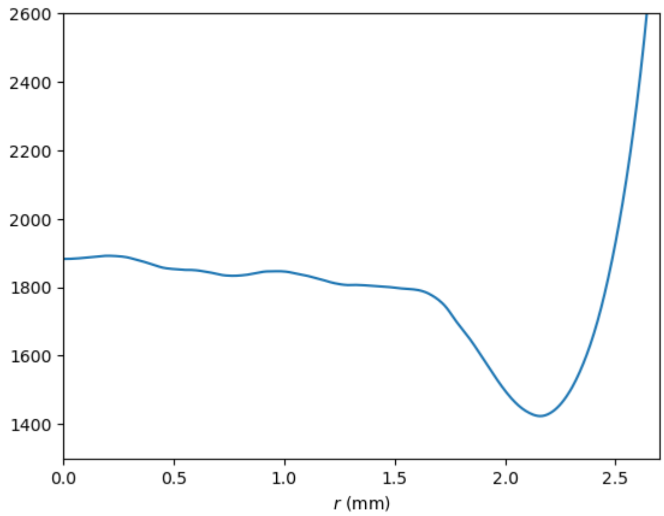

Figure 11: Profile of the Temperature

After applying Plank's law, we can obtain the temperature. The augmentation of the temperature at the end of the wing can be explained by the $J640/J750$ ratio in Plank's law that turns to 0/0 which tends to infinity in the end of the flame. Nevertheless, it is clearer on the profile of temperature.

In conclusion, the temperature remains stable in the flame at approximately 1900K, then it decreases down to 1400K to finally peak in the wing of the flame, as seen in figures 10 and 11.

8 Uncertainties

For this temperature to be valid, it is necessary to evaluate its uncertainty in order to ensure a precise result. Indeed, despite the strict protocol that we used and the quality equipment at our disposal, there still remain some measurement errors. Here, our main sources of uncertainty come from the wavelength filter and the deconvolution.

In order to calculate the uncertainty, we will use the following formula:

$$\frac{u(T)}{T} = \sqrt{(\frac{u(\lambda)}{\lambda})^2 + (\frac{u(J)}{J})^2} \tag{6}$$

With:

- u(T): the searched uncertainty in the temperature
- u(λ): the uncertainty in the wavelength
- u(J): the uncertainty related to the deconvolution

The uncertainty in the wavelength comes from the filter. Indeed the filter has a bandwidth of 10nm.

$\lambda \pm 10nm$ and u(λ) = 10nm

Thus, the captured wavelengths can go from 630nm to 650nm for the chosen wavelength at 640nm, and from 740nm to 760nm for the chosen wavelength at 750nm.

Now for the uncertainty of J, we know that we took 100 images for each wavelength and therefore made 100 deconvolutions, to then take an average of these images. However since this an average we need to take into account the standard deviation, but also the uncertainty of the Abel deconvolution. This is calculated thanks to Python.

We now have all the necessary values to calculate the uncertainty on T with:

$$u(T) = T * \sqrt{(\frac{u(\lambda 1)}{\lambda 1})^2 + (\frac{u(\lambda 2)}{\lambda 2})^2 + (\frac{u(J1)}{J1})^2 + (\frac{u(J2)}{J2})^2} \tag{7}$$

By writing this in the Python code, we obtained the following image, that represents the uncertainty depending on the part of the flame.

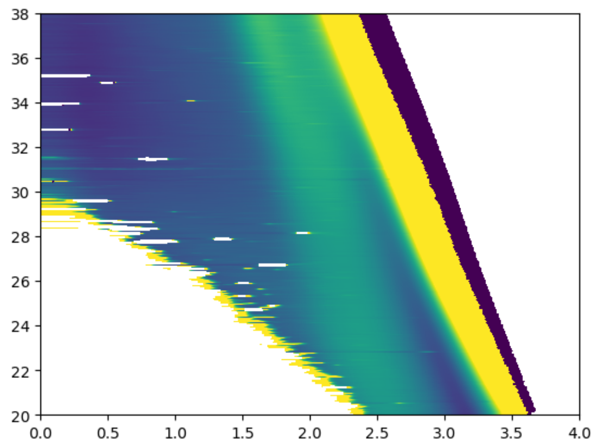

Figure 12: Uncertainty on T depending on location

This graph shows that for both wavelengths, the uncertainty on the temperature is way higher on the sides of the flame (yellow) than in the center (blue), since the flame isn't entirely stable while the 100 pictures are being taken. This way, we can say that the temperature found near the center of the flame is reliable but we need to be careful with the temperature found on the edges since it is not necessarily very accurate.

9 Conclusion

To conclude, this study focused on the concept of inverse problem and its various applications, with a particular focus on Abel inversion. Inverse problems play a crucial role in many scientific and technical fields, where we aim to deduce internal properties of a system from external measurements. Whether in medical imaging, geophysics, astrophysics or optics, these methods make it possible to reconstruct hidden or indirect information from observable data.

As part of our experiment, we applied Abel's inversion to retrieve the temperature of a flame, from its 2D picture. By taking photos of the flame at two different wavelengths, we were able to measure the light intensities emitted. These measurements were then processed by the Abel inversion method to reconstruct the flame temperature profile. Indeed, we were able to obtain the profile of the temperature as a function of the flame's radius. However, after evaluating the uncertainties of our experiment, we realized our results contain measurement errors. The accuracy of our results on the edges of the flame thus needs to be considered with doubt.

Nevertheless, the results of our experiment show that Abel inversion, like other inverse problem solving methods, remains a powerful tool in the analysis of complex phenomena. Our study illustrates its effectiveness in determining temperatures within a flame, with potential implications for other areas requiring precise reconstruction of internal profiles. Future improvements could include more precise filters and advanced inversion algorithms for better accuracy and reliability of results. Thus, the study of inverse problems continues to prove essential for the advancement of modern science and technology.

10 Acknowledgments

We would like to thank Mijail Littin, the supervising professor of this project. It is thanks to his pedagogy that we were able to successfully complete it. His support during the practical sessions and his explanations of the Inversion Problems as well as the expected results were essential to its smooth progress. We would also like to thank the CORIA Research Unity for allowing us to conduct the experiment in their laboratory.

References

[1] Deconvolution vs convolutions, dec 2023.

[2] Flame, 2024.

[3] Z. Dai, A. M. El-Leathy, K.-C. Lin, P. B. Sunderland, F. Xu, G. M. Faeth, D. L. Urban, and Z.-G. Yuan. *Laminar Soot Processes (LSP)*. PhD thesis, University of Michigan, 2002.

[4] Felipe Escudero, Mijail Littin, Rodrigo Demarco, Fengshan Liu, and Andrés Fuentes. Sooting properties of laminar coflow non-premixed ethylene/hydrogen flames influenced by water vapor addition to the oxidizer. *Fire Safety Journal*, 141:103997, dec 2023.

[5] Markus Juvonen, Rashmi Murthy, Tatiana Bubba, Luca Ratti, Rasmus Backholm, Salla Latva-Äijö, Alexander Meaney, and Siiri Rautio. Computational inverse problems. School: University of Helsinki.

[6] Mijail Littin. Inverse problems: Deriving hidden information from what we see. P6 Project Introduction Document, feb 2024.

[7] Jonathan M. Marr and Francis P. Wilkin. *A Better Presentation of Planck's Radiation Law*. PhD thesis, Union College, 2012.

[8] Tiangang Cui Nan Ye, Farbod Roosta-Khorasani. Optimization methods for inverse problems, dec 2017.

[9] Christopher R. Shaddix, Jiayao Zhao, and Timothy C. Williams. Soot concentration, temperature, and radiant emission measurements in a turbulent ethylene jet flame, nov 2019.

[10] PyAbel team. Comparison of abel transform methods, 2016.

[11] Jérôme Yon, Juan José Cruz, Felipe Escudero, José Morán, Fengshan Liu, and Andrés Fuentes. Revealing soot maturity based on multi-wavelength absorption/emission measurements in laminar axisymmetric coflow ethylene diffusion flames. *Combustion and Flame*, 227:147–161, may 2021.